JBC RESEARCH ARTICLE

N-acetylglucosaminyltransferase-V requires a specific noncatalytic luminal domain for its activity toward glycoprotein substrates

Received for publication, December 7, 2021, and in revised form, January 21, 2022 Published, Papers in Press, January 30, 2022,
https://doi.org/10.1016/j.jbc.2022.101666

Reina F. Osuka[1], Tetsuya Hirata[2], Masamichi Nagae[3,4], Miyako Nakano[5], Hiroyuki Shibata[6], Ryo Okamoto[6], and Yasuhiko Kizuka[1,2,*]

From the [1]Graduate School of Natural Science and Technology, and [2]Institute for Glyco-core Research (iGCORE), Gifu University, Gifu, Japan; [3]Department of Molecular Immunology, Research Institute for Microbial Diseases, and [4]Laboratory of Molecular Immunology, Immunology Frontier Research Center (IFReC), Osaka University, Suita, Japan; [5]Graduate School of Integrated Sciences for Life, Hiroshima University, Higashihiroshima, Japan; [6]Department of Chemistry, Graduate School of Science, Osaka University, Toyonaka, Japan

Edited by Gerald Hart

***N*-acetylglucosaminyltransferase-V (GnT-V or MGAT5) catalyzes the formation of an *N*-glycan β1,6-GlcNAc branch on selective target proteins in the Golgi apparatus and is involved in cancer malignancy and autoimmune disease etiology. Several three-dimensional structures of GnT-V were recently solved, and the recognition mechanism of the oligosaccharide substrate was clarified. However, it is still unclear how GnT-V selectively acts on glycoprotein substrates. In this study, we focused on an uncharacterized domain at the N-terminal side of the luminal region (N domain) of GnT-V, which was previously identified in a crystal structure, and aimed to reveal its role in GnT-V action. Using lectin blotting and fluorescence assisted cell sorting analysis, we found that a GnT-VΔN mutant lacking the N domain showed impaired biosynthetic activity in cells, indicating that the N domain is required for efficient glycosylation. To clarify this mechanism, we measured the *in vitro* activity of purified GnT-VΔN toward various kinds of substrates (oligosaccharide, glycohexapeptide, and glycoprotein) using HPLC and a UDP-Glo assay. Surprisingly, GnT-VΔN showed substantially reduced activity toward the glycoprotein substrates, whereas it almost fully maintained its activity toward the oligosaccharides and the glycopeptide substrates. Finally, docking models of GnT-V with substrate glycoproteins suggested that the N domain could interact with the substrate polypeptide directly. Our findings suggest that the N domain of GnT-V plays a critical role in the recognition of glycoprotein substrates, providing new insights into the mechanism of substrate-selective biosynthesis of *N*-glycans.**

The mammalian cell surface is covered with glycans that are structurally and functionally diverse and are often attached to proteins. Glycosylation is the most common posttranslational protein modification and critically regulates protein functions (1, 2). The vast majority of glycans attached to proteins are classified as *N*-, *O*-glycans, GPI-anchors, and *C*-mannose, and *N*-glycans are commonly found in eukaryotes (1, 3). *N*-Glycans are crucial for protein folding and localization (1) and regulate cell adhesion, cell–cell interactions, and signal transduction (4). Furthermore, changes in *N*-glycan structures are involved in development and exacerbation of various diseases, including cancer, diabetes, and Alzheimer's disease (5–7). Therefore, an understanding of how *N*-glycan structures are maintained and altered is important for the development of new therapies.

N-Glycans are biosynthesized by glycosyltransferases and glycosidases as proteins pass through the endoplasmic reticulum (ER) to the Golgi apparatus. *N*-Glycan biosynthesis in most eukaryotes starts with the transfer of the common triglucosylated glycan $Glc_3Man_9GlcNAc_2$ to an asparagine in the consensus sequence Asn-X-Ser/Thr by an oligosaccharyltransferase in the ER (1, 8). After the trimming of the Glc and Man residues, *N*-glycans are further modified by various glycosyltransferases in the Golgi to create more complex structures that include branching, extension, and capping. The *N*-glycan structures differ depending on the cell type, protein, and glycosylation site, and these differences enable the complex biological functions of glycoproteins. In particular, the high number of possible GlcNAc branches is unique to *N*-glycans and regulates the activity, stability, and localization of *N*-glycoproteins (6, 9). Although almost all the glycosyltransferase genes involved in mammalian *N*-glycan synthesis have been discovered and the detailed pathway of *N*-glycan biosynthesis has been clarified, the mechanisms responsible for how the activities of glycosyltransferases are regulated in cells and how the protein-specific structures of *N*-glycans are produced have not been elucidated.

In this study, we focused on *N*-acetylglucosaminyltransferase-V (GnT-V or MGAT5), which is the enzyme that catalyzes the formation of the β1,6-GlcNAc branch of *N*-glycans in the Golgi apparatus using UDP-GlcNAc as the donor substrate (10, 11) (Fig. 1*A*). N-acetylglucosaminyltransferase-V is highly related to cancer development and malignancy (12, 13). Transcription of the *MGAT5* gene is driven by the oncogenic

* For correspondence: Yasuhiko Kizuka, kizuka@gifu-u.ac.jp.

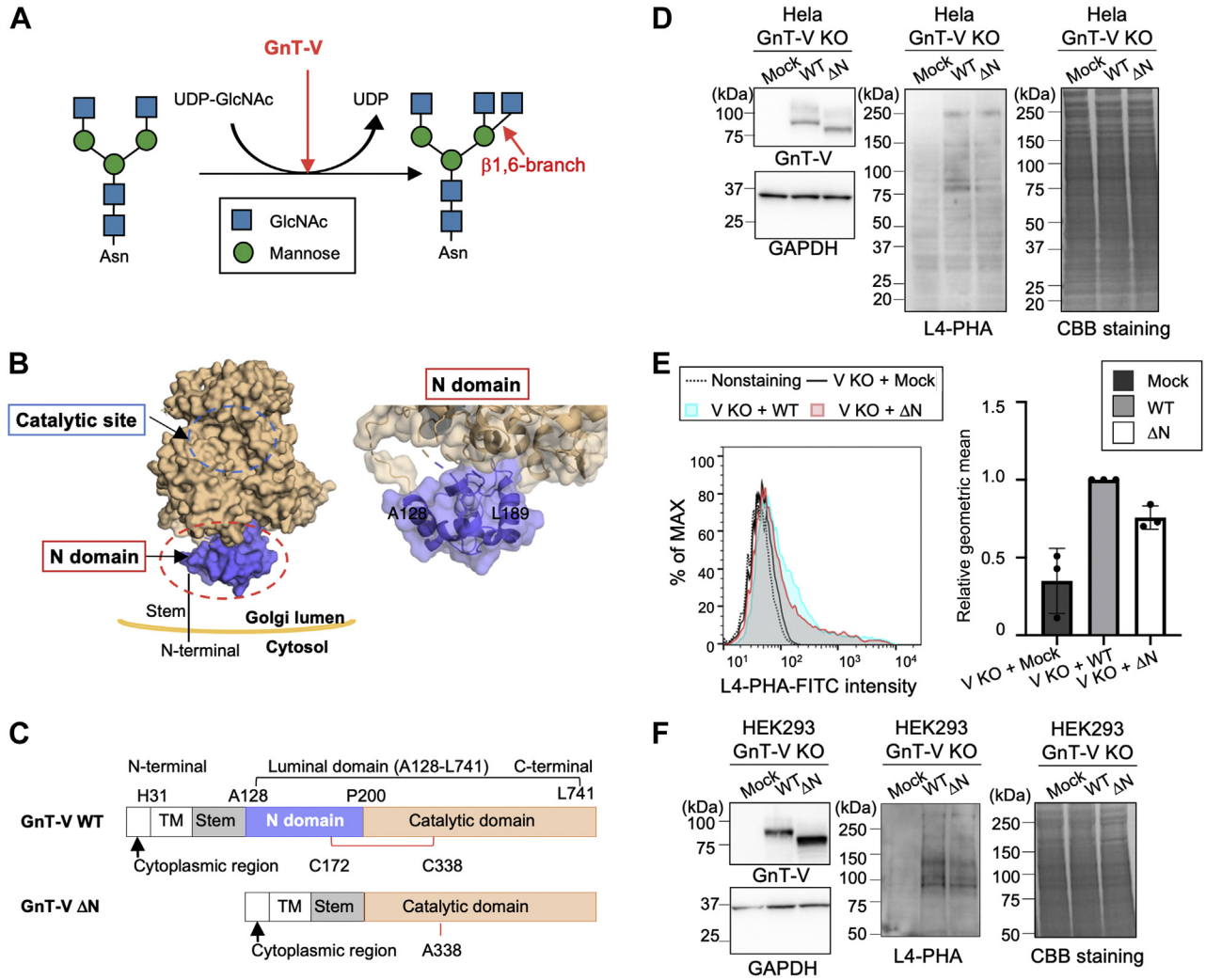

Figure 1. Intracellular activity of GnT-V WT and GnT-VΔN. *A*, schematic model of the GnT-V catalyzed reaction on *N*-glycan. *B*, the three-dimensional structure of the human GnT-V luminal region (*left*) and N domain (*right*). L189 (which corresponds to L188 of hamster GnT-V) is shown. *C*, plasmid constructs of GnT-V WT and GnT-VΔN. TM stands for transmembrane region. *D*, N-acetylglucosaminyltransferase-V WT or GnT-VΔN was expressed in HeLa GnT-V KO cells. The cellular proteins were separated by SDS-PAGE, followed by CBB staining or blotting with anti-GnT-V, anti-GAPDH, or L4-PHA lectin. *E*, *left*, FACS analysis of HeLa GnT-V KO cells with L4-PHA lectin. *Dotted line*, nonstained cells; *solid line*, stained mock-transfected cells; colored with *light blue*, GnT-V WT-expressing cells; colored with *orange*, GnT-VΔN-expressing cells. *Right*, the relative geometric means of L4-PHA-FITC signals are shown in the graph (n = 3). Three independent assays were carried out using different sets of transfected cells. *F*, N-acetylglucosaminyltransferase-V WT or GnT-VΔN was expressed in HEK293 GnT-V KO cells. The cellular proteins were separated by SDS-PAGE, followed by CBB staining or blotting with anti-GnT-V, anti-GAPDH, or L4-PHA lectin. GnT-V, N-acetylglucosaminyltransferase-V; L4-PHA, leukoagglutinating-phytohemagglutinin.

Ras–Raf–Ets pathway (14). N-acetylglucosaminyltransferase-V selectively modifies *N*-glycans on its target glycoproteins and glycosites, and the GnT-V-synthesized β1,6-GlcNAc branch impacts cell surface residency and clustering of growth factor receptors (15) and affects the adhesion activity of cadherins and integrins (16, 17), thereby promoting proliferation and metastasis of cancer cells. Furthermore, in GnT-V KO mice, cancer growth and metastasis are suppressed (12), and in human cancer patients, high expression of GnT-V and its product glycan are positively correlated with poor prognoses (18). These findings indicate that GnT-V is a promising drug target for cancer therapy and that elucidation of the mechanisms of how GnT-V acts on its target glycoproteins in cells will be critically important for understanding and manipulating GnT-V activity.

Similar to other glycosyltransferases, GnT-V has a type II membrane topology composed of a short N-terminal cytosolic region, a transmembrane domain, a stem region, and a large C-terminal catalytic region (19). The crystal structures of the luminal region of GnT-V solved by us and another group allowed the elucidation of the catalytic residue and the binding sites for the acceptor and donor substrates (20, 21). In addition, our recent study using a structural model of a GnT-V-substrate complex and a series of point mutants suggested that a few amino acid residues outside the catalytic pocket are involved in recognizing the glycan core or polypeptide part of the acceptor substrate (22). Furthermore, GnT-V was reported to show higher activity toward denatured glycoproteins than native ones (23). These results strongly suggest that the polypeptide moiety of the acceptor glycoprotein significantly

affects GnT-V activity, but how GnT-V recognizes and selects its glycoprotein substrates in cells remains unclear.

In several glycosyltransferases, the noncatalytic domains regulate the subcellular localization or acceptor preference (24–26). A previous study suggested that the stem region of GnT-V is involved in dimer formation (27). Furthermore, our analysis of the crystal structure of GnT-V found an uncharacterized domain next to the catalytic region (20). This domain (hereafter designated as the N domain), only found in GnT-V among the glycosyltransferases, is located at the N-terminal side of the catalytic domain and is comprised of approximately 80 amino acid residues with four α-helices (Fig. 1, *B* and *C*). Although the functions of the N domain have not been studied, a point mutation in this domain (L188R) in CHO mutant Lec4A cells caused abnormal accumulation of GnT-V in the ER, resulting in abolition of the biosynthesis of the β1,6-branch despite maintaining enzymatic activity toward an oligosaccharide substrate (24, 28). This demonstrates that the N domain is required for GnT-V function, but its precise roles are unclear.

In this study, we aimed to clarify the roles of the N domain in GnT-V. For this purpose, we made a GnT-V mutant lacking the N domain (GnT-VΔN) and investigated its activity and localization. We discovered that the GnT-V N domain is required for the activity toward glycoprotein substrates and efficient glycan biosynthesis in cells, highlighting a novel mechanism of GnT-V action in which GnT-V possibly acts on its target through recognition of acceptor proteins by the N domain.

Results

The N domain is required for efficient glycan biosynthesis by GnT-V in cells

To clarify the functions of the N domain in cells, first, an expression plasmid for GnT-VΔN was constructed. Our previous structural analysis of human GnT-V (hGnT-V) revealed that the N domain ranged from Ala128 to Pro200 (20) (Fig. 1*C*). It was also determined that Cys172 in the N domain formed a disulfide bond with Cys338 in the catalytic domain. Based on these findings, we designed a construct for GnT-VΔN in which the N domain (from Ala128 to Pro200) was deleted and Cys338 was mutated to Ala to avoid undesirable disulfide bonding. We confirmed that the mutation of Cys338 to alanine *per se* did not impair enzymatic activity of GnT-V (Fig. S1). To examine the activity of GnT-VΔN in cells, GnT-V WT and GnT-VΔN were expressed in HeLa GnT-V KO cells (22), and the cell lysates were analyzed by Western and lectin blotting. Our previous study found that exogenous expression of GnT-V in HeLa GnT-V KO cells restored the signals with leukoagglutinating-phytohemagglutinin (L4-PHA) lectin, which preferentially detects the β1,6-branch (29), enabling us to evaluate the biosynthetic activity of expressed GnT-V (22). Compared with mock-treated cells, the signals of L4-PHA in GnT-V WT-expressing cells were increased (Fig. 1*D*, first and second lanes), confirming the specificity of L4-PHA. Although the level of GnT-VΔN in cells was almost equal to GnT-V WT, the L4-PHA signals in ΔN-expressing cells were lower than those in GnT-V WT-expressing cells (Fig. 1*D*, second and third lanes). To investigate this further, the expression levels of the β1,6-branch on the cell surface were compared using fluorescence assisted cell sorting (FACS) (Fig. 1*E*). Again, the expression of GnT-V WT in HeLa GnT-V KO cells restored the reactivity with L4-PHA (Fig. 1*E*, light blue), and the L4-PHA-signals of ΔN-expressing cells were lower than WT-expressing cells (Fig. 1*E*, orange, 75.6% of WT-expressing cells). These results indicate that the N domain is needed for the efficient biosynthesis of the β1,6-branch in cells. To explore whether the N domain is generally required for efficient biosynthesis in various cell types, we established HEK293 GnT-V KO cells and performed similar experiments. Knockout of *MGAT5* gene was validated by genotyping PCR and the GnT-V activity assay using HPLC (Fig. S2). As a result, compared with GnT-V WT, GnT-VΔN produced a lower amount of the L4-PHA-reactive β1,6-branch in HEK293 GnT-V KO cells (Fig. 1*F*). We also carried out FACS analysis using HEK293 GnT-V KO cells. Signals of ZsGreen1, whose cDNA was inserted downstream GnT-V-IRES2 (Fig. S3*A*), confirmed the similar transfection efficiency between WT and ΔN (Fig. S3*B*). Again, L4-PHA-Rhodamin signals were lower in GnT-VΔN-expressing cells than GnT-V WT-expressing cells (Fig. S3*C*). Together, these findings suggest that the N domain is required for the full intracellular activity of GnT-V.

The N domain is dispensable for the enzyme activity of GnT-V toward glycan substrates

Considering that glycan synthesis was impaired in GnT-VΔN-expressing cells, we reasoned that the N domain is either directly involved in the GnT-V reaction or indirectly involved in glycan biosynthesis by regulating GnT-V behaviors such as localization or complex formation. First, we examined whether the N domain is required for GnT-V catalytic activity toward glycan substrates. To this end, GnT-V WT and GnT-VΔN were individually expressed in HeLa GnT-V KO cells, and enzyme assays were performed using the cell lysates as enzyme sources. As acceptor substrates, two kinds of fluorescence-labeled biantennary *N*-glycan oligosaccharides, GnGnbi-2-aminopyridine (PA) and GnGnbi-Asn-PNSNB (N-(2-(2-pyridylamino)ethyl)succinamic acid 5-norbornene-2,3-dicarboxyimide ester), were used (Fig. 2*A*), both of which serve as GnT-V substrates (22). The reaction mixtures were analyzed by HPLC, and the activities of GnT-V WT and GnT-VΔN were calculated based on the peak area of the GnT-V products (Fig. 2*A*). As a result, the GnT-VΔN activity was almost equal to that of GnT-V WT toward both oligosaccharide substrates (Fig. 2*B*), demonstrating that the N domain is not directly involved in the GnT-V catalytic reaction. To confirm these results, soluble His6-tagged GnT-V WT and GnT-VΔN, that lack the cytoplasmic and transmembrane regions (Fig. 2*C*), were expressed and purified for use in the enzyme assays. Coomassie brilliant blue (CBB) staining was used to confirm the purity of both enzymes (Fig. 2*D*). The activity assays using the

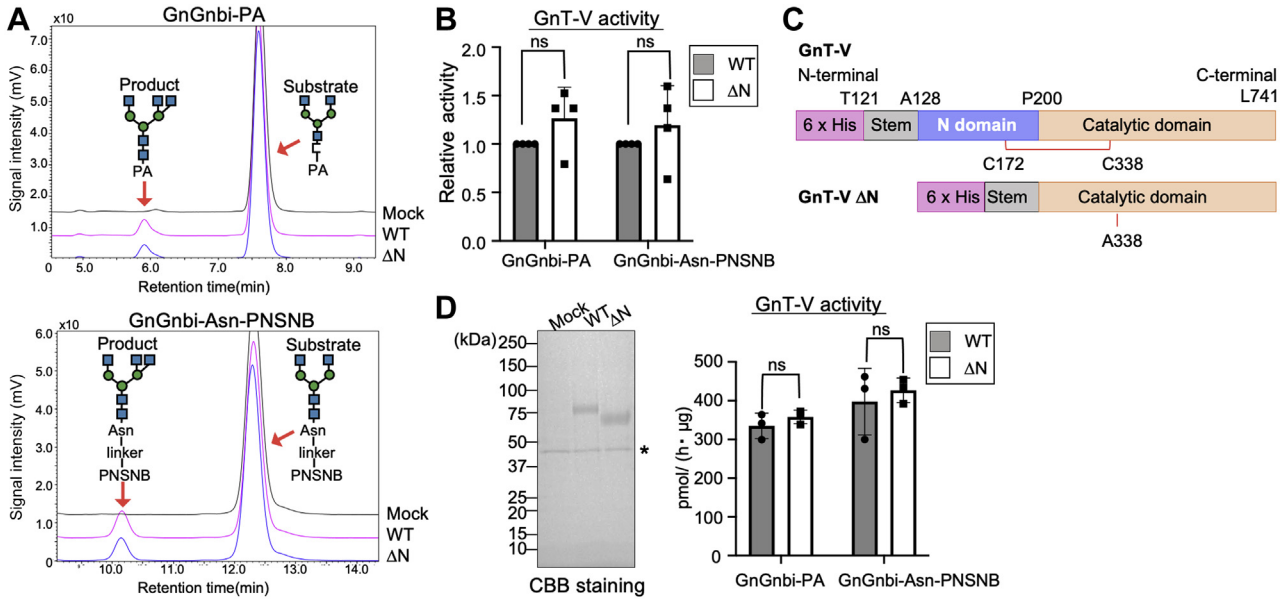

Figure 2. Enzyme activity of GnT-V WT and ΔN toward oligosaccharide substrates. *A*, lysates of HeLa cells expressing GnT-V WT or ΔN were reacted with GnGnbi-PA or GnGnbi-Asn-PNSNB as the oligosaccharide acceptor. The acceptor substrates and the GnT-V products were separated using reverse-phase HPLC. *B*, the activity of GnT-V WT or ΔN calculated by the peak area in (*A*) (n = 4, means ± S.D.). The samples were collected from independent sets of transfected cells. The *p* value was calculated by Holm-Sidak's test. N.S., not significant. *C*, plasmid constructs of soluble GnT-V WT and ΔN used in this study. *D*, *left*, soluble GnT-V WT or ΔN was expressed in COS7 cells and purified from the culture supernatants using Ni^{2+}-beads. Purified GnT-V WT or ΔN was separated by SDS-PAGE and stained with CBB. *non-specific band. *Right*, the activity of purified soluble GnT-V WT or ΔN was measured, same as (*A*) (n = 3, mean ± S.D.). Three independent assays were carried out using the same purified enzymes. The *p* value was calculated by 2-way ANOVA and multiple *t* test. N.S., not significant. GnT-V, N-acetylglucosaminyltransferase-V; PA, 2-aminopyridine; PNSNB, (N-(2-(2-pyridylamino)ethyl)succinamic acid 5-norbornene-2,3-dicarboxyimide ester).

purified enzymes again showed that the activity of the soluble form of GnT-VΔN was comparable to that of soluble GnT-V WT for both oligosaccharide substrates. Taken together, these data clearly show that the N domain is dispensable for the enzyme activity toward oligosaccharide substrates.

The N domain deletion partially affects the intracellular localization of GnT-V

Next, we examined whether the N domain regulates the intracellular localization of GnT-V. To investigate the subcellular localization of GnT-V WT and ΔN in cells, immunofluorescence staining was carried out (Fig. 3*A*). Both GnT-V WT and ΔN were localized in the Golgi apparatus and also in other compartments, but a difference in localization between WT and ΔN was not clearly observed in this analysis.

To further examine potential difference in the subcellular localization of GnT-V WT and ΔN, sucrose density gradient fractionation experiments were carried out. Homogenates of HeLa GnT-V KO cells expressing GnT-V WT or ΔN were fractionated by sucrose density gradient from 10 to 45%, and GnT-V and the organelle markers were analyzed by Western blotting (Fig. 3*B*). Both GnT-V WT and ΔN were mainly detected in fractions 2 to 5, and the Golgi marker GM130 was also highly observed in fractions 3 to 5 (Fig. 3*B*), suggesting that both GnT-V WT and ΔN were localized in the Golgi apparatus as well as in other compartments. In more detail, GnT-V WT showed a broad peak in fractions 2 to 5, whereas the highest signals of GnT-VΔN were observed in fractions 2 to 3. As fractions 1 to 2 contain the ER and lysosome markers, this suggested that the subcellular localization of GnT-VΔN was partially shifted to the ER or lysosomes. We also performed the same fractionation experiments using HEK293 GnT-V KO cells and found that the position of GnT-VΔN was shifted from that of GnT-V WT, suggesting that GnT-VΔN was more localized in nonGolgi compartments than GnT-V WT (Fig. S4). Considering that GnT-VΔN retained catalytic activity almost equal to the WT toward glycan substrates in enzyme assays (Fig. 2), GnT-VΔN is likely folded and is unlikely to be entrapped in the ER.

In addition to the results of subcellular localization, previous study showed that GnT-V can be cleaved at the juxtamembrane region in the Golgi apparatus and secreted to the extracellular space (30, 31). We speculated that the increase in nonGolgi localization of GnT-VΔN might lead to a decrease in secretion. To test this possibility, GnT-V WT and ΔN were expressed in HeLa GnT-V KO cells, and the cellular and secreted proteins were analyzed by Western blotting. As a result, the amount of GnT-VΔN in the medium was comparable to that of GnT-V WT (Fig. 3*C*). Collectively, these data suggest that deletion of the N domain has effects on intracellular localization but not on secretion of GnT-V.

The N domain is essential for the GnT-V enzyme activity toward the glycoprotein substrate

Our enzyme assays and localization analyses above showed that GnT-VΔN retains enzyme activity toward oligosaccharide substrates (Fig. 2) and displayed a partial change in localization

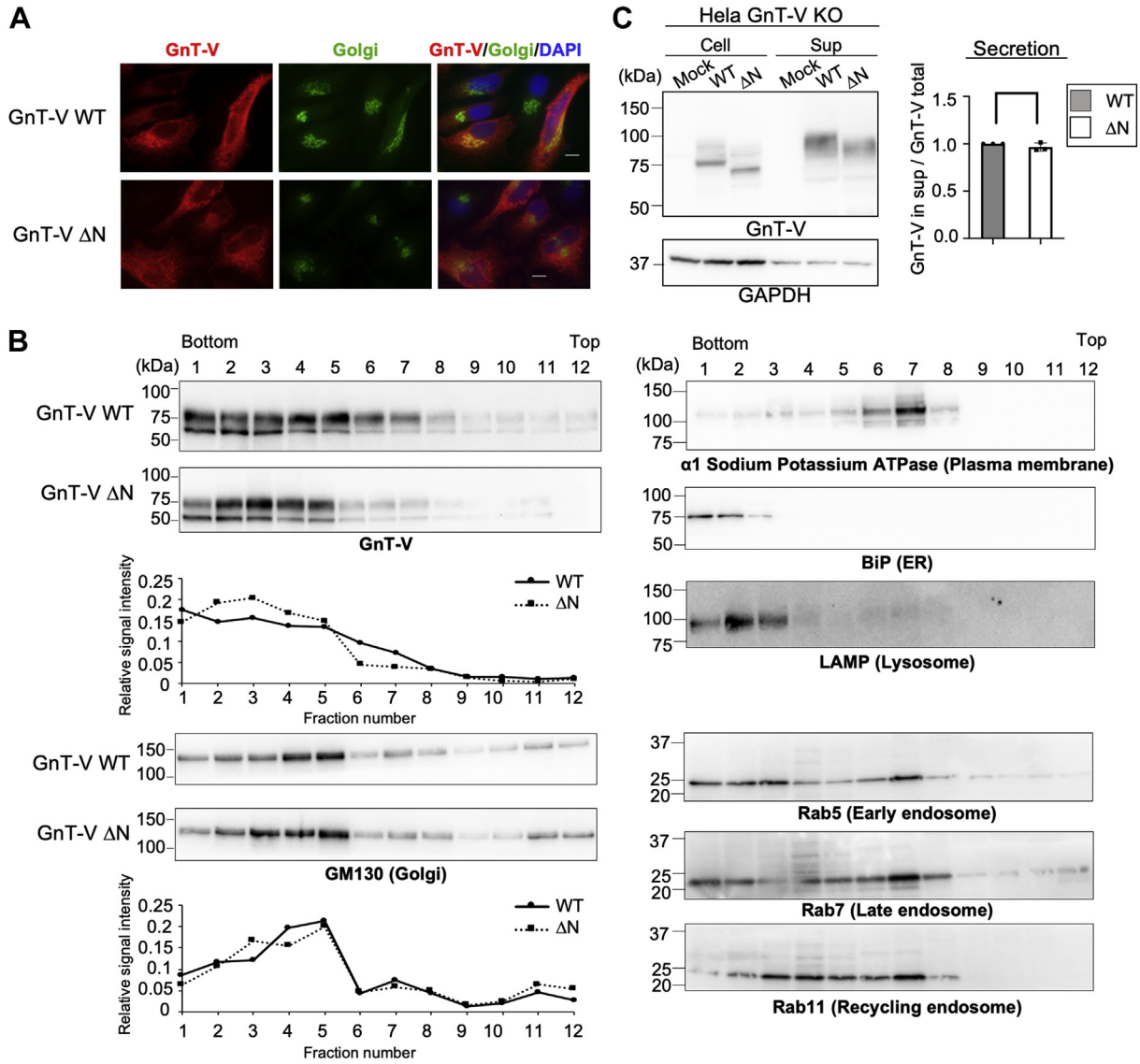

Figure 3. Intracellular localization of GnT-V WT and GnT-VΔN. *A*, HeLa cells transfected with GnT-V WT or ΔN were stained with anti-GnT-V (*red*), anti-Golgin97 (*green*), and DAPI (*blue*). The scale bar represents 10 μm. *B*, homogenates of HeLa GnT-V KO cells were subjected to 10 to 45% (w/v) sucrose density gradient fractionation. The proteins in each fraction were separated by SDS-PAGE and blotted with antibodies for GnT-V and organelle markers. The graphs displayed the relative signals of GnT-V or GM130 in each fraction. *C*, full length GnT-V WT or ΔN was expressed in HeLa GnT-V KO cells. The cellular proteins (cell) and secreted proteins in the culture supernatants (sup) were separated by SDS-PAGE and immunoblotted with anti-GnT-V and anti-GAPDH (*left*). The ratios of secreted/total GnT-V signals, relative to that of GnT-V WT, are shown in the graph (*right*) (n = 3, mean ± S.D.). The *p* value was calculated by Welch's *t* test. DAPI, 4′,6-diamidino-2-phenylindole; GnT-V, N-acetylglucosaminyltransferase-V.

(Fig. 3), which is unlikely to be the primary reason for the reduced glycan biosynthesis in cells. Based on these findings, we hypothesized that GnT-VΔN is defective in recognizing glycoprotein substrates. To investigate the activity toward glycoprotein substrates, we performed UDP-Glo assays (32). As the levels of UDP (a byproduct of the glycosylation reaction) are measured in UDP-Glo assay, this system can be used to quantify and compare glycosyltransferase activity toward any type of acceptor substrate. Human serum-derived alpha-1-acid glycoprotein (α1AGP), transferrin, and recombinant human superoxide dismutase 3 (SOD3) purified from HEK293 GnT-V KO cells were used as the glycoprotein substrates. As a glycopeptide substrate, chicken egg yolk-derived sialylglycohexapeptide (SGP) was used. First, all the glycoprotein and glycopeptide substrates were treated with neuraminidase and β-galactosidase to remove terminal sialic acid and galactose residues because the presence of these residues in an *N*-glycan almost completely inhibits the GnT-V reaction (10, 20). Removal of sialic acid by neuraminidase was confirmed by the reduced reactivity of *Sambucus sieboldiana* agglutinin (SSA) lectin, which recognizes α2,6-sialic acid (33), and the concomitant increased reactivity of *Ricinus communis* agglutinin (RCA) lectin, which recognizes terminal galactose (34) (Fig. 4*A*). The increased RCA reactivity disappeared after further treatment with β-galactosidase, and the protein bands stained with CBB were reduced in size in a step-wise fashion by neuraminidase and β-galactosidase treatments (Fig. 4*A*), confirming that the glycans of the substrate glycoproteins were

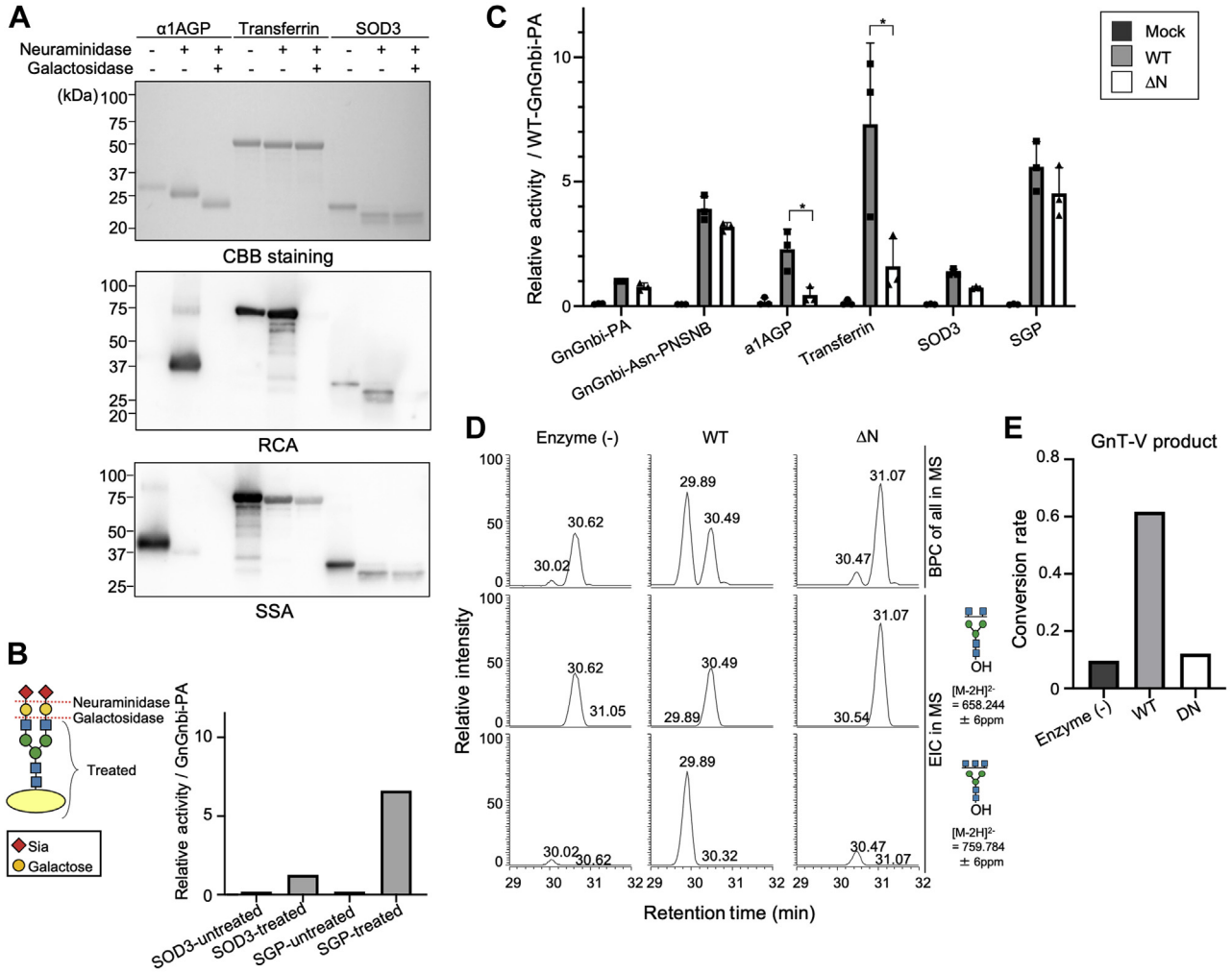

Figure 4. The *in vitro* activity of soluble GnT-V WT and ΔN toward various substrates measured by the UDP-Glo assay. *A*, treatment of the glycoproteins used in this assay with sialidase and galactosidase. The treated proteins were stained with CBB, SSA, or RCA lectin. *B*, schematic diagram of substrate preparation by glycosidase treatments for the UDP-Glo assay (*left*). The UDP-Glo assay was performed using purified soluble GnT-V WT and glycosidase-treated or -untreated substrates (SOD3 or SGP) (*right*). *C*, comparison of the *in vitro* activity of GnT-V WT and GnT-VΔN toward various types of substrates using the UDP-Glo assay. The relative activity toward each substrate was evaluated by setting the activity of GnT-V WT toward GnGnbi-PA as 1 (n = 3, mean ± S.D. *$p < 0.05$). The *p* value was calculated by 2-way ANOVA Dunnett's test. *D*, base peak chromatogram (BPC) from LC-ESI-MS analysis of *N*-glycans from transferrin which had been incubated with GnT-V WT, ΔN, or vehicle. Extracted ion chromatograms (EICs) of the substrate biantennary glycan and the product triantennary glycan are also shown. *E*, the ratios of signal intensity of the product glycan to that of total (substrate + product) glycans in (*D*) are shown. GnT-V, N-acetylglucosaminyltransferase-V; PA, 2-aminopyridine; RCA, Ricinus communis agglutinin; SGP, chicken egg sialylglycopeptide; SOD3, superoxide dismutase 3; SSA, Sambucus sieboldiana agglutinin.

trimmed as expected. Therefore, we conducted the UDP-Glo enzyme assays using these prepared substrates and purified soluble GnT-V WT and ΔN. Considering the number of *N*-glycans attached to each acceptor substrate, the same amount of *N*-glycan (100 pmol) was added to each reaction. Using GnT-V WT, we first found that the glycosidase treatments dramatically increased the signals for both glycoprotein (SOD3) and glycohexapeptide (SGP) substrates (Fig. 4*B*), indicating that this assay system in combination with the glycosidase treatment can be used to measure GnT-V activity toward various substrates. Next, the enzyme activity of GnT-VΔN was compared with that of GnT-V WT toward six substrates, including oligosaccharides (GnGnbi-PA and GnGnbi-Asn), glycoproteins (α1AGP, transferrin, and SOD3) and a glycohexapeptide (SGP). As a result, the enzyme activity of GnT-VΔN toward the oligosaccharide substrates was almost equal to that of GnT-V WT (Fig. 4*C*), consistent with the above assay results using HPLC (Fig. 2, *B* and *D*). Similarly, GnT-VΔN showed comparable activity as WT toward the glycohexapeptide SGP. However, the activity of GnT-VΔN toward glycoproteins was found to be remarkably less than that of GnT-V WT for all three glycoproteins.

To directly confirm that GnT-VΔN produced less amounts of the product glycan on glycoproteins than GnT-V WT, we performed LC-MS analysis of transferrin *N*-glycans after the *in vitro* reactions by GnT-V WT and ΔN (Fig. S5). As a standard glycoprotein, bovine fetuin, whose glycan structures were already determined (35), was also analyzed after desialylation and degalactosylation (Fig. S5*B*). After incubation with GnT-V WT and ΔN, the enzymatic product triantennary glycan was detected in transferrin *N*-glycans (Figs. 4*D* and S5*A*), and the ratios of peak intensity of the biantennary glycan

(substrate) and the triantennary glycan (product) were shown (Fig. 4*E*). The conversion rate of GnT-VΔN was drastically decreased compared with that of GnT-V WT, consistent with the results of UDP-Glo assay. These findings showed that the N domain is vital for the enzyme activity toward glycoprotein substrates, even though it is unnecessary for recognition of the glycan substrate itself.

To investigate whether N domain is required for the activity toward any glycoprotein, we prepared a small monomeric glycoprotein (CCL1) bearing a single *N*-glycan by chemical synthesis (Fig. S6, *A* and *B*). UDP-Glo assay revealed that GnT-V WT showed activity toward CCL1 comparable to that toward an oligosaccharide (GnGnbi-PA) acceptor, and ΔN fully retained activity toward CCL1 (Fig. S6*C*). This suggests that glycan modification of not all glycoproteins require N domain of GnT-V and that ΔN can act on small monomeric glycoproteins.

Docking models of GnT-V with glycoprotein substrates

Finally, to provide structural insights into how the N domain is involved in the recognition of glycoprotein substrates, we generated docking models of GnT-V with glycoproteins (α1AGP, transferrin, SOD3, or CCL1) or SGP (Fig. 5). The N domain is linked to the catalytic domain through two flexible loops (Fig. 5, green dotted circles) (20). Furthermore, the positions of the glycoproteins are also flexible because of the conformational flexibility of glycans. Consequently, the N domain may directly interact with the glycoproteins, particularly for large glycoproteins. By contrast, in the model of CCL1 and SGP, substrates for which the WT and ΔN have almost equal enzyme activity (Figs. 4*C* and S6*C*), the peptide part is too far from the N domain to interact with it (Fig. 5, *D* and *E*). These data suggest that the N domain could stabilize the GnT-V-substrate complex by interacting with the glycoprotein substrate.

Discussion

In this study, we discovered that the N domain of GnT-V, which is located at its luminal side, is essential for its activity toward glycoprotein substrates, but not toward oligosaccharides, and is needed for efficient biosynthesis of glycans in cells. These findings indicated that GnT-V does not simply modify the glycan part of any *N*-glycoprotein but rather selectively acts on target proteins by recognizing their polypeptides, providing new insights into how various *N*-glycoforms are produced in cells in a protein-dependent manner. There are some reports showing that glycosyltransferases act in a protein-dependent manner. For instance, α1,6-fucosyltransferase, the enzyme responsible for core fucosylation (36, 37), could accept oligomannose glycans on erythropoietin but not on ribonuclease B (38). In addition, UDP-GlcNAc:lysosomal enzyme GlcNAc-1-phosphotransferase, which is responsible for mannose-6-phosphate biosynthesis, has alpha and gamma subunits that are involved in the recognition of lysosomal enzymes (39).

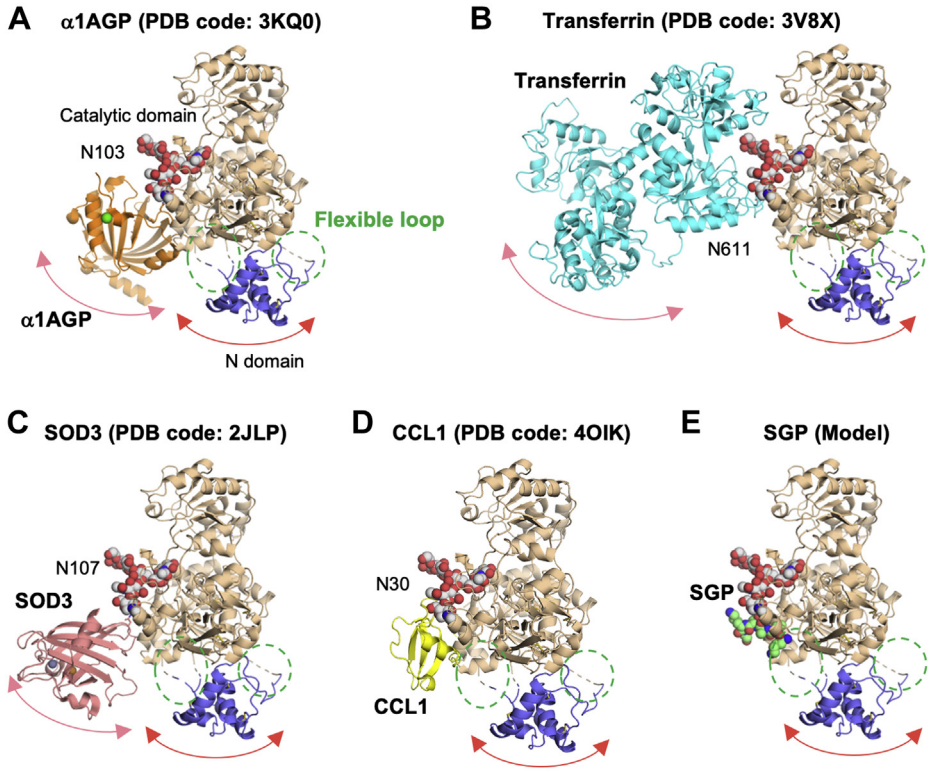

Figure 5. Docking model of GnT-V and glycoprotein substrates. Structural models of GnT-V complexed with *N*-glycosylated α1AGP (PDB, 3KQ0) (*A*), transferrin (PDB, 3V8X) (*B*), SOD3 (PDB, 2JLP) (*C*), CCL1 (PDB, 4OIK) (*D*), and SGP (*E*). The N domain is connected to the catalytic region *via* two flexible loops (*green dotted circles*). *N*-Glycans on these glycoproteins (or peptide) have the biantennary GlcNAc-terminated structure (GnGnbi) shown in *sphere models*. α1AGP, alpha-1-acid glycoprotein; GnT-V, N-acetylglucosaminyltransferase-V; SGP, chicken egg sialylglycopeptide; SOD3, superoxide dismutase 3.

These findings, together with ours in this study, indicate that the sequence or structure of acceptor proteins potentially affects structures of *N*-glycans synthesized in cells.

In our enzyme assay, the activity of GnT-VΔN toward oligosaccharides was almost equal to that of WT. This is consistent with previous study in which GnT-V mutants lacking a part of the N domain fully retained their activity toward oligosaccharides (27). In addition, a soluble GnT-V catalytic domain that lacks the whole N domain and was used for structural studies is still active toward oligosaccharides (20, 21). These data demonstrated that the N domain is not involved in a monosaccharide transfer reaction itself. Instead, our UDP-Glo data clearly showed that the N domain of GnT-V is required for its action toward glycoprotein substrates. However, in contrast to the substantial reduction of enzyme activity of ΔN in UDP-Glo assay, we observed slight (20∼30%) reduction in lectin reactivity in cell experiments (Fig. 1). This discrepancy might be triggered by the different experimental conditions, and overexpression of the enzymes in cell experiments might compensate for the lower activity of GnT-VΔN in cells.

We also found that GnT-VΔN exists more in nonGolgi compartments compared with WT (Fig. 3), suggesting that the N domain could also regulate GnT-V localization. A previous study has shown that a point mutation in the N domain (L188R) drastically changed the localization of GnT-V from the Golgi to the ER (24). The mutation of lysine to arginine at residue 188 likely disrupts the hydrophobic pocket of the N domain, which could make the whole structure unstable, likely resulting in the entrapment of the transferase in the ER. Similarly, deletion of the N domain might also partially retain GnT-V in the ER. As ER-resident GnT-V is likely nonfunctional because of the absence of its acceptor substrate glycans, the decrease of glycan biosynthesis in GnT-VΔN-expressing cells might be partially caused by the altered localization of GnT-VΔN. Although it is unclear how GnT-V is transported from the ER to the Golgi, a regulatory protein might recognize the N domain and assist in its transport. The N domain has a weak similarity with the CARD domain, which is a module for protein–protein interactions (40). This suggests that the N domain of GnT-V may also bind with another protein for GnT-V transport. Future studies should include experiments that will help to elucidate how GnT-V is trafficked to the Golgi and whether the GnT-V N domain binds to an intracellular protein to assist its transport.

In the UDP-Glo assay, we found that GnT-VΔN was less active than GnT-V WT toward glycoprotein substrates but not toward oligosaccharides and a glycohexapeptide (Fig. 4), strongly suggesting that GnT-V prefers limited types of aglycones as acceptors depending on the N domain. The acceptor preference of GnT-V may be related to the number of glycosites, the size, and the specific sequence or 3D motif of the substrates. The two oligosaccharide substrates, SGP, and CCL1 are all singly *N*-glycosylated, and these four substrates were almost equally modified by GnT-V WT and ΔN. By contrast, the rest of glycoprotein substrates have multiple glycosylation sites (five for α1AGP (41) and two for transferrin (42)) or form a homo-oligomer (SOD3 comprised of singly *N*-glycosylated monomers (43)). As these glycoprotein substrates were modified favorably by GnT-V WT but poorly by GnT-VΔN, multiple *N*-glycans in a substrate might enhance GnT-V action through its N domain. In addition to the number of glycosites, the size of acceptor protein may be important for the action of GnT-V, as glycan modification of the smaller glycoproteins, SOD3 and CCL1, was less affected by the deletion of N domain. The third possibility is a preferred sequence or 3D motif exists within the substrate proteins. As GnT-VΔN is unable to act very efficiently on most of the glycoproteins used in our UDP-Glo assay, a specific glycoprotein 3D structure, amino acid sequence, or 3D motif might be recognized by GnT-V WT. Previous study revealed that GnT-V showed higher activity toward denatured glycoproteins than native ones, and the accessibility or exposure of specific sequence motifs was suggested as a factor for recognition by GnT-V (23). In contrast, in our UDP-Glo assay using a specific glycoprotein, we found that GnT-V showed almost the same activity toward native and heat-treated α1AGP (Fig. S6*D*). It is important to examine in the future whether GnT-V recognizes a specific sequence or motif. The acceptor sugars in oligosaccharide substrates are likely to be highly accessible to GnT-V, but in our assay, the GnT-V activity toward GnGnbi-PA was not higher than its activity toward glycoproteins, suggesting that accessibility toward the acceptor sugars is not the dominant factor for GnT-V action toward glycoproteins. Future work should include activity assays using other types of glycoproteins to provide more information regarding the aglycone selectivity of GnT-V.

Regarding the role of the N domain in GnT-V-mediated catalysis, there are two possibilities. One is that the N domain could interact with substrate proteins directly, leading to stable interactions between substrate and enzyme. In our docking models of GnT-V and acceptor glycoproteins, the N domain was near enough to interact with the substrate proteins, but not with the short peptide of SGP, based on their positions and flexibilities. The other possibility is that the N domain could change the conformation of the catalytic domain by moving like a pendulum. As the N domain is connected to the neighboring domain *via* two highly flexible loops (19, 21), movement of the N domain might alter the conformation of the catalytic region for efficient product release. However, if this putative conformational change induced by the N domain is a prerequisite for GnT-V action, GnT-VΔN would lose activity regardless of the type of substrate. As GnT-VΔN showed similar activity as the WT toward oligosaccharide substrates (Figs. 2 and 4), the former possibility is likely more feasible. To examine this point further, cocrystallization of GnT-V with a glycoprotein substrate will be helpful.

In addition to the GnT-V N domain, noncatalytic accessory domains in glycosyltransferases have also been reported to participate in glycosylation reactions. For instance, α1,6-fucosyltransferase has a unique Src homology 3 domain that is essential for recognizing the glycan substrate and forming a complex with an oligosaccharyltransferase subunit (25).

Moreover, a stem region of protein *O*-linked mannose β1,2-N-acetylglucosaminyltransferase 1, which synthesizes the GlcNAc-β1, 2-Man-Ser/Thr structure, has lectin activity and recognizes its product glycan (44). The interaction between the stem region and the product may help to facilitate glycosylation at multiple sites in a substrate molecule or recruit another enzyme to form a complex with protein *O*-linked mannose β1,2-N-acetylglucosaminyltransferase 1 (45). The discovery of these domains suggests that various glycosyltransferases could have distinct accessory domains to promote their reactions or select their targets.

In conclusion, this study revealed that N domain is essential for GnT-V full activity and gives insights into how GnT-V selectively acts on glycoprotein substrates. Because GnT-V is a therapeutic target for cancer and immune-related diseases (12, 15, 18), elucidation of the detailed regulation mechanisms of the GnT-V reaction could lead to the development of new glycan-targeted drugs. Furthermore, in general, it is unclear how glycans are synthesized in cells in a protein-dependent manner, and recent findings including ours suggest that protein-dependent glycosylation could be partly mediated by the accessory domains of glycosyltransferases. Understanding the roles of uncharacterized noncatalytic domains and regulatory factors of glycosyltransferases will contribute to the elucidation of mammalian glycosylation mechanisms, leading to new strategies to modify protein glycosylation.

Experimental procedures

Reagents

The following antibodies and lectins were used: anti-GnT-V (mouse, clone 706824, R&D Systems), anti-α1 sodium potassium ATPase (mouse, clone 464.6, Abcam), anti-LAMP1 (rabbit, Abcam), anti-GAPDH (mouse, clone 6C5, Merck Millipore), anti-GRP78 (BiP) (rabbit, Abcam), anti-GM130 (rabbit, clone D6B1) (Cell Signaling Technology), anti-Golgin97 (rabbit, clone D8P2K, Cell Signaling Technology), anti-Rab5 (rabbit, clone C8B1, Cell Signaling Technology), anti-Rab7 (rabbit, Cell Signaling Technology), anti-Rab11 (rabbit, Cell Signaling Technology), horseradish peroxidase (HRP)-conjugated anti-mouse IgG (GE Healthcare), HRP-conjugated anti-rabbit IgG (GE Healthcare), unconjugated-L4-PHA (J-Chemical), biotinylated-SSA (J-Chemical), biotinylated-RCA (Vector Laboratories), FITC-conjugated L4-PHA (J-Oil Mills), Rhodamine-conjugated L4-PHA (Vector Laboratories), Alexa546-conjugated anti-mouse IgG (Invitrogen), Alexa488-conjugated anti-rabbit IgG (Invitrogen). L4-PHA was conjugated to HRP using a Peroxidase Labeling Kit-NH2 (Dojindo) as described previously (22).

Structure representation

All three-dimensional structures used for docking models (GnT-V:5ZIB and 5ZIC, *N*-glycan: 4BM7, α1AGP:3KQ0, transferrin: 3V8X, SOD3: 2JLP, and CCL1: 4OIK) were retrieved from the Protein Data Bank. Rotamer modification of glycosylated asparagine was manually performed by COOT (46). Structural superposition was performed by LSQKAB (47). The hypothetical model of the glycohexapeptide (NH2-Lys-Val-Ala-Asn-Lys-Thr-COOH) was built based on a similar peptide sequence (PDB code: 4OWT) by COOT. All figures were rendered by PyMOL (The PyMOL Molecular Graphics System, Version 2.0 Schrödinger, LLC).

Plasmid construction

Construction of pcDNA6 myc-His A/human GnT-VΔN was carried out in two steps. First, the two DNA fragments encoding parts of human GnT-V (from the N terminus to Val127 and from Trp201 to the C terminus) were amplified by PCR using pcDNA6 myc-His A/human GnT-V as the template and the primers listed in Table S1. The amplified DNA fragments were ligated to the NotI/XhoI sites of pcDNA6 myc-His A using the NEBuilder HiFi DNA Assembly Master Mix (New England Biolabs) according to the manufacturer's protocol. Next, to substitute Cys338 with Ala, the plasmid constructed above was mutated using the QuickChange Lightning Site-Directed Mutagenesis Kit (Agilent Technologies) according to the manufacturer's protocol. Similarly, pcDNA6 myc-His A/human GnT-V C338A was constructed using pcDNA6 myc-His A/human GnT-V as the template. The plasmid for His6-tagged soluble GnT-VΔN (pcDNA-IH/GnT-VΔN) was constructed in two steps as follows. Using the QuickChange Lightning Site-Directed Mutagenesis Kit and pcDNA-IH/human GnT-V as a template, a point mutation was introduced at residue 338 to convert Cys to Ala. Then, the DNA fragment that encodes the immunoglobulin kappa-chain signal sequence, His6 tag, and the part of human GnT-V (from Thr121 to Val127) was amplified by PCR using pcDNA-IH/human GnT-V C338A as a template. Another DNA fragment encoding a part of GnT-V (from Trp201 to Leu741) was also amplified by PCR as in the case of pcDNA6 myc-His A/human GnT-VΔN. These two fragments were ligated to pcDNA-IH, which had been digested with XhoI and KpnI, using the NEBuilder HiFi DNA Assembly Master Mix according to the manufacturer's protocol. To construct pTK-hGnT-V-IRES2-ZsGreen1, the linearized pTK-hGnT-V sequence was obtained by PCR using pTK-hGnT-V (22) as the template and the IRES2-ZsGreen1 sequence was amplified by PCR using pIRES2-ZsGreen1 (Takara) as the template. The amplified sequences were ligated using NEBuilder HiFi DNA Assembly Master Mix. For construction of pTK-hGnT-VΔN, the DNA fragment encoding GnT-VΔN was amplified by PCR using pcDNA6 myc-His A/human GnT-VΔN as the template. The amplified fragment was ligated to the XhoI/XbaI sites of pTK-hGnT-V-IRES2-ZsGreen1 using the NEBuilder HiFi DNA Assembly Master Mix. The two pX330-puro plasmids encoding the sgRNAs for the human *MGAT5* gene were generated as described previously (22).

Cell culture

COS7, HeLa, HeLa GnT-V KO, and HEK293 GnT-V KO cells were cultured in Dulbecco's modified Eagle's medium (DMEM) containing 10% fetal bovine serum and 50 μg/ml kanamycin under 5% CO_2 conditions at 37 °C. The GnT-V KO

HEK293 cell clone was established by a CRISPR system as in the case of the HeLa GnT-V KO cells as described previously (22). In brief, HEK293 cells were transfected with two pX330-puro plasmids targeting two sites in the *MGAT5* gene, followed by selection with puromycin for 2 days. The selected cells were subjected to limiting dilution and a *MGAT5* genotype of each cell clone was examined by PCR. Knockout of the *MGAT5* gene in the clone (#10) used in this study was confirmed by PCR and a GnT-V activity assay (Fig. S2).

Plasmid transfection

Cells at 60 to 80% confluency on a 6-cm (or 10-cm) dish were transfected with 4 μg (or 10 μg) of plasmids using Lipofectamine 3000 Reagent (Thermo Fisher Scientific) according to the manufacturer's protocol. The cells were collected 48 h after transfection and used for subsequent experiments.

Western and lectin blotting, and CBB staining

Cells were washed with PBS and collected by centrifugation at 470*g* for 3 min and at 13,800*g* for 1 min. The cells were lysed with lysis buffer (50 mM Tris–HCl (pH 7.4), 150 mM NaCl, 1% Nonidet P-40) and sonicated. The protein concentrations of the cell lysates were measured using the Pierce BCA Protein Assay Kit (Thermo Fisher Scientific), according to the manufacturer's protocol. To prepare the samples for SDS-PAGE, the lysates were mixed with Laemmli 5× SDS sample buffer and boiled at 95 °C for 5 min. The same amount of protein was loaded into each lane of the SDS-PAGE, and the proteins were resolved by 5 to 20% SDS-PAGE. For CBB staining of the gel, the proteins were stained with GelCode Blue Safe Protein Stain (Thermo Fisher Scientific). For Western blotting, the separated proteins were transferred to nitrocellulose membranes using a semi-dry blotter. The membranes were blocked with 5% skim milk in Tris-buffered saline (TBS) containing 0.1% Tween-20 (TBS-T) and incubated with primary antibodies diluted with 5% skim milk in TBS-T overnight at 4 °C. After washing with TBS-T for 5 min three times, the membranes were incubated with HRP-conjugated secondary antibodies at room temperature for 1 h. For blotting with HRP-lectins, after transfer, the membranes were blocked with 1% bovine serum albumin (BSA) in TBS-T overnight at 4 °C, followed by incubation at room temperature for 30 min with HRP-conjugated lectins that were diluted with 1% BSA in TBS-T. For blotting with biotinylated lectins, the membranes were incubated with TBS-T overnight at 4 °C for blocking, followed by incubation at room temperature for 30 min with biotinylated lectins that were diluted with TBS-T. The membranes were incubated with the VECTASTAIN ABC Standard kit (Vector Laboratories) (1:400 in TBS-T) at room temperature for 30 min. Proteins were detected with the Western Lightning Plus-ECL (PerkinElmer) or SuperSignal West Femto Maximum Sensitivity Substrate (Thermo Fisher Scientific) using a FUSION-SOLO 7s EDGE (Vilber Lourmat). Antibodies and lectins were diluted as follows: anti-GnT-V (1:2000), anti-α1 sodium potassium ATPase (1:500), anti-GAPDH (1:2000), anti-GRP78 (1:500), anti-GM130 (1:300), anti-LAMP1 (1:300), anti-Rab5 (1:300), anti-Rab7 (1:300), anti-Rab11 (1:300), HRP-conjugated anti-mouse IgG (1:5000), HRP-conjugated anti-rabbit IgG (1:20,000), biotinylated-SSA (1:2000), biotinylated-RCA (1:2000), and HRP-conjugated L4-PHA (1:5000). Representative images of three or more experiments are shown in the figures.

FACS analysis

Cells cultured on 10-cm dishes were transfected and scraped for collection after 48 h, followed by washing with PBS twice. Then, the cells were centrifugated and suspended in FACS buffer (1% BSA and 0.1% NaN_3 in PBS) for blocking. The cells were centrifuged again and incubated with L4-PHA-FITC (1: 250) or L4-PHA-Rhodamine (1:200) in FACS buffer on ice for 15 min for staining molecules at the cell surface. Signals were detected using a BD FACSMelody cell sorter (BD Bioscience), and the data were analyzed using FlowJo (FlowJo LLC).

Purification of recombinant proteins

To obtain soluble His6-tagged GnT-V and GnT-VΔN, COS7 cells were cultured on 15-cm dishes. When confluency reached 60 to 80%, the cells were transfected with the plasmids using polyethyleneimine MAX (Polyscience). After 4 h, the medium was replaced with Opti-MEM I, followed by further incubation for 72 h. The media containing soluble His6-tagged GnT-V and its mutants were incubated with Ni^{2+}-Sepharose 6 Fast Flow (GE Healthcare) for 3 h or more by gentle rotation. After washing the beads three times with 10 mM phosphate buffer (pH 7.4) containing 20 mM imidazole and 0.5 M NaCl, the recombinant proteins were eluted with 10 mM phosphate buffer (pH 7.4) containing 0.5 M NaCl and 0.5 M imidazole (elution buffer). The eluates were diluted with elution buffer so that the enzyme concentrations were the same between WT and GnT-VΔN and were directly used as the enzyme source. Preparation of His6-tagged hSOD3 was performed in almost the same way as that of His6-tagged GnT-V except HEK293 GnT-V KO cells were used instead of COS7 cells.

N-acetylglucosaminyltransferase-V activity assay using HPLC

N-acetylglucosaminyltransferase-V activity toward oligosaccharide substrates was measured using HPLC as described previously (22). In this assay, the fluorescence-labeled oligosaccharides GnGnbi-PA and GnGnbi-Asn-PNSNB were used as substrates, and the cell lysates or purified soluble His6-tagged GnT-V and its mutants were used as enzyme sources. Briefly, the enzyme source was incubated at 37 °C in 10 μl of the reaction buffer that contained 100 μM acceptor substrate, 20 mM UDP-GlcNAc, 125 mM MES (pH 6.25), 10 mM EDTA, 200 mM GlcNAc, 0.5% (v/v) Triton X-100, and 1 mg/ml BSA. After 1 h, the GnT-V reaction was stopped by boiling at 99 °C for 2 min. Then, the mixture was diluted with 40 μl of water, followed by centrifugation at 21,000*g* for 3 min. The supernatant was analyzed by reverse-phase HPLC with an ODS column (TSKgel ODS-80TM, TOSOH Bioscience, 4.6 × 150 mm). High-pressure liquid chromatography analysis was

conducted in the isocratic mode in which buffer A (20 mM ammonium acetate buffer (pH 4.0)) and buffer B (1% butanol in buffer A) were mixed in a proportion of five to one.

Preparation of the acceptor substrate for the UDP-Glo assay

Human α1AGP (G9885, Sigma), human transferrin apoform (transferrin) (Wako), and chicken egg SGP (α2,6-SGP) (Fushimi) were purchased and used for the assays. A total of 500 μg of α1AGP, transferrin, or SGP was digested with 0.25 unit/ml of *Arthrobacter ureafaciens* neuraminidase (Nacalai Tesque) and 80 unit/ml of *Streptococcus pneumoniae* β-galactosidase (New England Biolabs) in 87 mM sodium acetate buffer (pH 4.5) at 37 °C overnight. For heat denaturation, glycosidase-treated α1AGP was incubated at 60, 80, or 100 °C for 10 min.

Chemical synthesis of CCL1

The synthesis of CCL1 was carried out as previously described (48) with slight modifications. The details of the synthesis are now in preparation for submitting elsewhere.

N-acetylglucosaminyltransferase-V activity assay using UDP-Glo

The UDP-Glo assay was performed using a UDP-Glo Glycosyltransferase Assay kit (Promega) as described previously (22). Briefly, the GnT-V reaction was conducted in a 96-well white plate by incubating the purified GnT-V or its mutants with acceptor substrates for 2 h at room temperature in 10 μl of the reaction mixture that contained 10 mM ultrapure UDP-GlcNAc (supplied in the kit), an acceptor substrate, 125 mM MES (pH 6.25), 10 mM EDTA, 200 mM GlcNAc, 0.5% (v/v) Triton X-100, and 1 mg/ml BSA. The concentrations of the acceptor substrates were defined so that 100 pmol of *N*-glycans were added per well based on the number of *N*-glycans they have (α1AGP, 5; transferrin, 2; SOD3, 1; CCL1, 1; and SGP, 1). After the reaction, 15 μl of the GnT-V buffer (125 mM MES (pH 6.25), 10 mM EDTA, 0.5% (v/v) Triton X-100, and 1 mg/ml BSA) was added to each well followed by adding 25 μl of the UDP detection reagent (supplied in the kit). Then, the plate was incubated in the dark for 1 h at room temperature. Chemiluminescence signals were measured using a SYNERGY H1 microplate reader (BioTek). The duplicate measurements for each sample were performed, and the independent experiments were repeated at least three times for each acceptor substrate.

Glycan structural analysis by LC-MS

Purified GnT-V WT or ΔN was mixed with transferrin in the reaction buffer same as that used in UDP-Glo assay (100 pmol of *N*-glycans were included for each reaction). As a negative control, the elution buffer (described in "Purification of recombinant proteins") was added instead of the enzyme solution. After the mixtures were incubated at 37 °C for 30 min, the samples were mixed with Laemmli 5× SDS sample buffer and boiled at 95 °C for 5 min. The reaction mixtures containing transferrin were separated by SDS-PAGE. The proteins on the gel were transferred to a PVDF membrane, and the membrane was dried at room temperature for 5 h. The membrane was washed once with ethanol for 1 min and then three times with water for 1 min each. The proteins on the membrane were stained for 5 min with Direct Blue 71 (800 μl of solution A: 0.1% (w/v) Direct Blue 71 (Sigma-Aldrich) in 10 ml of solution B: acetic acid: ethanol: water = 1:4:5). After destaining the membrane with solution B for 1 min, the membrane was dried at room temperature overnight. The transferrin bands were excised from the membrane and then placed in 100 μl of 1% (w/v) poly(vinylpyrrolidone) 40,000 in 50% (v/v) methanol in separate wells of a 96-well microtiter plate, and agitated for 20 min, and then washed with water (100 μl × five times). The release of *N*-glycans from transferrin by peptide *N*-glycosidase F (PNGase F), reduction into alditol *N*-glycans, and desalting using a cation-exchange column were all performed according to the method of Nakano *et al.* (49) with some modifications. The alditol *N*-glycans were analyzed by LC-MS according to our previously reported procedure (5). Briefly, alditol *N*-glycans were separated on a carbon column (5 μm HyperCarb, 1 mm I.D. × 100 mm, Thermo Fisher Scientific) using an Vanquish HPLC pump (flow rate: 50 μl/min, column oven: 40 °C) under the following gradient conditions involving a sequence of isocratic and two segmented linear gradients: 0 to 8 min, 10 mM NH_4HCO_3; 8 to 38 min, 6.75 to 15.75% (v/v) acetonitrile in 10 mM NH_4HCO_3; 38 to 73 min, 15.75 to 40.5% (v/v) acetonitrile in 10 mM NH_4HCO_3; increasing to 81% (v/v) acetonitrile in 10 mM NH_4HCO_3 for 7 min; and re-equilibrated with 10 mM NH_4HCO_3 for 15 min. The eluate was continuously introduced into an ESI source (LTQ Orbitrap XL, Thermo Fisher Scientific). Mass spectrometry (MS) spectra were obtained in the negative ion mode using Orbitrap MS (mass range m/z 500 to m/z 2500; capillary temperature: 300 °C, source voltage: 3.0 kV; capillary voltage: −18 V; tube lens voltage: −112.80 V). Xcalibur software ver. 2.2. (Thermo Fisher Scientific) was used to analyze MS data and to show the base peak chromatogram and extracted ion chromatogram. Monoisotopic masses were assigned with possible monosaccharide compositions using the GlycoMod software tool (mass tolerance for precursor ions is ±0.006 Da, https://web.expasy.org/glycomod/).

Immunofluorescence staining

Cells seeded on an 8-well glass chamber slide were transfected with 0.4 μg of plasmid using lipofectamine 3000 Transfection Reagent. After 48 h, the cells were washed with PBS and fixed with 4% PFA/PBS. The cells were washed with PBS again, permeabilized, and blocked with PBS containing 0.1% digitonin (Fujifilm) and 3% BSA for 30 min at room temperature. After washing with PBS, the cells were incubated with primary antibodies, followed by incubation with Alexa488- or Alexa546-conjugated secondary antibodies and 4′,6-diamidino-2-phenylindole. Fluorescence signals were visualized using a BZX-800 all-in-one fluorescence microscope (KEYENCE). Antibodies were diluted as follows: anti-GnT-V (1:2000), anti-Golgin97 (1:500), Alexa546-conjugated anti-

mouse IgG (1:1000), and Alexa488-conjugated anti-rabbit IgG (1:1000).

Fractionation by sucrose density gradient centrifugation

Cells seeded on 15-cm dishes were transfected with 30 μg of plasmids using polyethyleneimine MAX. After 48 h, the cells were washed with PBS three times and collected. The cells were resuspended with 2 ml of 8.5% (w/v) sucrose in 10 mM Tris–HCl (pH 7.49) and homogenized on ice using a Potter-type tissue grinder (2 cm^3) and approximately 50 strokes. The cell homogenates were centrifuged at 500*g* for 5 min at 4 °C to remove nuclei and unbroken cells. A total of 1 ml of the supernatant was collected and used for fractionation. To prepare the sucrose gradient, 6.5 ml of 45% (w/v) sucrose solution (10 mM Tris–HCl (pH 7.49)) was first added to the bottom of a 13.2 ml ultracentrifuge tube, and 6.5 ml of 10% (w/v) sucrose solution (10 mM Tris–HCl (pH 7.49)) was overlaid. A continuous sucrose gradient of 10% (w/v) to 45% (w/v) was made using a Gradient Master (BioComp Instruments, Inc). After forming the gradient, 700 μl of the sucrose solution was removed from the top, and 1 ml of the cell homogenate was loaded. The tubes were centrifuged using a SW 41 Ti rotor (Beckmann Coulter) at 120,000*g* for 18 h at 4 °C with no brake. A total of 12 fractions (1 ml each) were collected using a peristaltic pump (ATTO). Each fraction was diluted with 1.6 ml of PBS and ultracentrifuged at 200,000*g* for 1 h at 4 °C to precipitate the membranes. The pellets were lysed with 40 μl of lysis buffer (50 mM Tris–HCl (pH 7.4), 150 mM NaCl, and 1% Nonidet P-40) and incubated on ice for 30 min. After incubation, the lysates were mixed with 5× SDS sample buffer and boiled at 95 °C for 5 min for SDS-PAGE.

Preparation of secreted proteins by ethanol precipitation

Cells were cultured on 6-cm dishes and transfected with the plasmids for GnT-V and its mutant. After 4 h, the medium was replaced with Opti-MEM I. After 48 h, the medium and cells were collected individually. The cell samples were prepared the same as described above (see "Western and lectin blotting, and CBB staining"). For the secreted proteins, the medium was first centrifuged at 400*g* for 5 min at 4 °C to remove cell debris. The supernatant was centrifuged at 3900*g* for 30 min at 4 °C through an Amicon Ultra-4 10K (Merck) to concentrate the samples. A total of 2.5 vol of 100% EtOH and 1/30 vol of 5 M NaCl were added to the samples, followed by incubation for 10 min at −80 °C. To precipitate the proteins, the sample was centrifuged at 13,500*g* for 20 min at 4 °C. The pellet was washed with 70% ethanol, followed by centrifugation at 13,500*g* for 5 min at 4 °C. The precipitated proteins were dissolved in lysis buffer (50 mM Tris–HCl (pH 7.4), 150 mM NaCl, and 1% Nonidet P-40) and sonicated. The samples were mixed with 5× SDS sample buffer and boiled at 95 °C for 5 min for SDS-PAGE.

Statistical analysis

Statistical analyses were performed using GraphPad Prism 8 software (GraphPad Software, Inc).

Data availability

Glycomic raw data for glycan-structure analysis have been deposited to the GlycoPOST (announced ID: GPST000231). All the other data are contained in the article. All the other data are contained within the article.

Supporting information—This article contains supporting information.

Acknowledgments—We thank Ms Chizuko Yonekawa, Yuko Tokoro, and Emiko Mori (Gifu University) for their technical help. We also thank Dr Yasuhiro Kajihara (Osaka University) for valuable and critical comments on this article. We thank Renee Mosi, PhD, from Edanz (https://jp.edanz.com/ac), for editing a draft of this article.

Author contributions—R. F. O., T. H., Masamichi Nagae, Miyako Nakano, H. S., and R. O. investigation; R. F. O. writing–original draft; T. H. and Y. K. supervision; Y. K. conceptualization; Y. K. writing–review and editing; Y. K. project administration; Y. K. funding acquisition.

Funding and additional information—This work was partially supported by a Grant-in-Aid for Scientific Research (B) to Y. K. [20H03207], a Leading Initiative for Excellent Young Researchers (LEADER) project (Y. K.) from the Japan Society for the Promotion of Science (JSPS), a CREST grant ([18070267] to Y. K.) from JST, a grant from the Takeda Science Foundation to Y. K., Nagoya University CIBoG program from MEXT WISE program to R. F. O., and a grant from the Tokyo Biochemical Research Foundation to Y. K.

Conflict of interest—The authors declare that they have no conflicts of interest with the contents of this article.

Abbreviations—The abbreviations used are: α1AGP, alpha-1-acid glycoprotein; BSA, bovine serum albumin; CARD, caspase recruitment domain; CBB, Coomassie brilliant blue; ER, endoplasmic reticulum; FACS, fluorescence assisted cell sorting; GnT-V, N-acetylglucosaminyltransferase-V; hGnT-V, human GnT-V; HRP, horseradish peroxidase; L4-PHA, leukoagglutinating-phytohemagglutinin; MS, mass spectrometry; PA, 2-aminopyridine; PNGase F, peptide *N*-glycosidase F; RCA, *Ricinus communis* agglutinin; SGP, chicken egg sialylglycopeptide; SOD3, superoxide dismutase 3; SSA, *Sambucus sieboldiana* agglutinin; TBS, Tris-buffered saline.

References

1. Schjoldager, K. T., Narimatsu, Y., Joshi, H. J., and Clausen, H. (2020) Global view of human protein glycosylation pathways and functions. *Nat. Rev. Mol. Cell Biol.* **21**, 729–749
2. Varki, A. (2017) Biological roles of glycans. *Glycobiology* **27**, 3–49
3. Moremen, K. W., Tiemeyer, M., and Nairn, A. V. (2012) Vertebrate protein glycosylation: Diversity, synthesis and function. *Nat. Rev. Mol. Cell Biol.* **13**, 448–462
4. Taniguchi, N., and Korekane, H. (2011) Branched N-glycans and their implications for cell adhesion, signaling and clinical applications for cancer biomarkers and in therapeutics. *BMB Rep.* **44**, 772–781
5. Kizuka, Y., Kitazume, S., Fujinawa, R., Saito, T., Iwata, N., Saido, T. C., Nakano, M., Yamaguchi, Y., Hashimoto, Y., Staufenbiel, M., Hatsuta, H., Murayama, S., Manya, H., Endo, T., and Taniguchi, N. (2015) An aberrant sugar modification of BACE 1 blocks its lysosomal targeting in Alzheimer's disease. *EMBO Mol. Med.* **7**, 175–189

6. Kizuka, Y., and Taniguchi, N. (2016) Enzymes for N-glycan branching and their genetic and nongenetic regulation in cancer. *Biomolecules* **6**, 25
7. Ohtsubo, K., Takamatsu, S., Minowa, M. T., Yoshida, A., Takeuchi, M., and Marth, J. D. (2005) Dietary and genetic control of glucose transporter 2 glycosylation promotes insulin secretion in suppressing diabetes. *Cell* **123**, 1307–1321
8. Aebi, M. (2013) N-linked protein glycosylation in the ER. *Biochim. Biophys. Acta* **1833**, 2430–2437
9. Boscher, C., Dennis, J. W., and Nabi, I. R. (2011) Glycosylation, galectins and cellular signaling. *Curr. Opin. Cell Biol.* **23**, 383–392
10. Gu, J., Nishikawa, A., Tsuruoka, N., Ohno, M., Yamaguchi, N., Kangawa, K., and Taniguchi, N. (1993) Purification and characterization of UDP-N-acetylglucosamine: -6-D-mannoside ß-6N-acetylglucosaminyltransferase(N-acetylglucosaminyltransferase V) from a human lung cancer cell line. *J. Biochem.* **113**, 614–619
11. Shoreibah, M., Perng, G. S., Adler, B., Weinstein, J., Basu, R., Cupples, R., Wen, D., Browne, J. K., Buckhaults, P., Fregien, N., and Pierce, M. (1993) Isolation, characterization, and expression of a cDNA encoding N- acetylglucosaminyltransferase V. *J. Biol. Chem.* **268**, 15381–15385
12. Granovsky, M., Fata, J., Pawling, J., Muller, W. J., Khokha, R., and Dennis, J. W. (2000) Suppression of tumor growth and metastasis in Mgat5-deficient mice. *Nat. Med.* **6**, 306–312
13. Pinho, S. S., and Reis, C. A. (2015) Glycosylation in cancer: Mechanisms and clinical implications. *Nat. Rev. Cancer* **15**, 540–555
14. Kang, R., Saito, H., Ihara, Y., Miyoshi, E., Koyama, N., Sheng, Y., and Taniguchi, N. (1996) Transcriptional regulation of the N-acetylglucosaminyltransferase V gene in human bile duct carcinoma cells (HuCC-T1) is mediated by Ets-1. *J. Biol. Chem.* **271**, 26706–26712
15. Demetriou, M., Granovsky, M., Quaggin, S., and Dennis, J. W. (2001) Negative regulation of T-cell activation and autoimmunity by Mgat5 N-glycosylation. *Nature* **409**, 733–739
16. Carvalho, S., Catarino, T. A., Dias, A. M., Kato, M., Almeida, A., Hessling, B., Figueiredo, J., Gartner, F., Sanches, J. M., Ruppert, T., Miyoshi, E., Pierce, M., Carneiro, F., Kolarich, D., Seruca, R., *et al.* (2016) Preventing E-cadherin aberrant N-glycosylation at Asn-554 improves its critical function in gastric cancer. *Oncogene* **35**, 1619–1631
17. Zhao, Y., Nakagawa, T., Itoh, S., Inamori, K. I., Isaji, T., Kariya, Y., Kondo, A., Miyoshi, E., Miyazaki, K., Kawasaki, N., Taniguchi, N., and Gu, J. (2006) N-acetylglucosaminyltransferase III antagonizes the effect of N-acetylglucosaminyltransferase V on α3β1 integrin-mediated cell migration. *J. Biol. Chem.* **281**, 32122–32130
18. Murata, K., Miyoshi, E., Kameyama, M., Ishikawa, O., Kabuto, T., Sasaki, Y., Hiratsuka, M., Ohigashi, H., Ishiguro, S., Ito, S., Honda, H., Takemura, F., Taniguchi, N., and Imaoka, S. (2000) Expression of N-acetylglucosaminyltransferase V in colorectal cancer correlates with metastasis and poor prognosis. *Clin. Cancer Res.* **6**, 1772–1777
19. Nagae, M., Yamaguchi, Y., Taniguchi, N., and Kizuka, Y. (2020) 3D structure and function of glycosyltransferases involved in N-glycan maturation. *Int. J. Mol. Sci.* **21**, 1–23
20. Nagae, M., Kizuka, Y., Mihara, E., Kitago, Y., Hanashima, S., Ito, Y., Takagi, J., Taniguchi, N., and Yamaguchi, Y. (2018) Structure and mechanism of cancer-associated N-acetylglucosaminyltransferase-V. *Nat. Commun.* **9**, 3380
21. Darby, J. F., Gilio, A. K., Piniello, B., Roth, C., Blagova, E., Hubbard, R. E., Rovira, C., Davies, G. J., and Wu, L. (2020) Substrate engagement and catalytic mechanisms of N-acetylglucosaminyltransferase V. *ACS Catal.* **10**, 8590–8596
22. Hirata, T., Nagae, M., Osuka, R. F., Mishra, S. K., Yamada, M., and Kizuka, Y. (2020) Recognition of glycan and protein substrates by N-acetylglucosaminyltransferase-V. *Biochim. Biophys. Acta Gen. Subj.* **1864**, 129726
23. Do, K. Y., Fregien, N., Pierce, M., and Cummings, R. D. (1994) Modification of glycoproteins by N-acetylglucosaminyltransferase V is greatly influenced by accessibility of the enzyme to oligosaccharide acceptors. *J. Biol. Chem.* **269**, 23456–23464
24. Weinstein, J., Sundaram, S., Wang, X., Delgado, D., Basil, R., and Stanley, P. (1996) A point mutation causes mistargeting of Golgi GlcNAc-TV in the Lec4A Chinese hamster ovary glycosylation mutant. *J. Biol. Chem.* **271**, 27462–27469
25. Tomida, S., Takata, M., Hirata, T., Nagae, M., Nakano, M., and Kizuka, Y. (2020) The SH3 domain in the fucosyltransferase FUT8 controls FUT8 activity and localization and is essential for core fucosylation. *J. Biol. Chem.* **295**, 7992–8004
26. Tu, L., Tai, W. C. S., Chen, L., and Banfield, D. K. (2008) Signal-mediated dynamic retention of glycosyltransferases in the Golgi. *Science* **321**, 404–407
27. Sasai, K., Ikeda, Y., Tsuda, T., Ihara, H., Korekane, H., Shiota, K., and Taniguchi, N. (2001) The critical role of the stem region as a functional domain responsible for the oligomerization and Golgi localization of N-acetylglucosaminyltransferase V. The involvement of a domain homophilic interaction. *J. Biol. Chem.* **276**, 759–765
28. Chaney, W., Sundaram, S., Friedman, N., and Stanley, P. (1989) The Lec4A CHO glycosylation mutant arises from miscompartmentalization of a Golgi glycosyltransferase. *J. Cell Biol.* **109**, 2089–2096
29. Yamamoto, K., Tsuji, T., and Osawa, T. (1993) Analysis of asparagine-linked oligosaccharides by sequential lectin-affinity chromatography. *Methods Mol. Biol.* **14**, 17–34
30. Kuhn, P. H., Voss, M., Haug-Kröper, M., Schröder, B., Scheperse, U., Bräse, S., Haass, C., Lichtenthaler, S. F., and Fluhrer, R. (2015) Secretome analysis identifies novel signal peptide peptidase-like 3 (Sppl3) substrates and reveals a role of Sppl3 in multiple golgi glycosylation pathways. *Mol. Cell. Proteomics* **14**, 1584–1598
31. Voss, M., Künzel, U., Higel, F., Kuhn, P., Colombo, A., Fukumori, A., Haug-Kröper, M., Klier, B., Grammer, G., Seidl, A., Schröder, B., Obst, R., Steiner, H., Lichtenthaler, S. F., Haass, C., *et al.* (2014) Shedding of glycan-modifying enzymes by signal peptide peptidase-like 3 (SPPL 3) regulates cellular N-glycosylation. *EMBO J.* **33**, 2890–2905
32. Rodriguez, A. C., Yu, S. H., Li, B., Zegzouti, H., and Kohler, J. J. (2015) Enhanced transfer of a photocross-linking N-acetylglucosamine (GlcNAc) analog by an O-GlcNAc transferase mutant with converted substrate specificity. *J. Biol. Chem.* **290**, 22638–22648
33. Takesada, H., Shibuya, N., and Nagashima, N. (1992) The interaction of elderberry (Sambucus sieboldiana) bark lectin and sialyloligosaccharides as detected by 1H-NMR. *J. Biochem.* **112**, 143–146
34. Rutenber, E., and Robertus, J. D. (1991) Structure of ricin B-chain at 2.5 Å resolution. *Proteins* **10**, 260–269
35. Green, E. D., Adelt, G., Baenziger, J. U., Wilson, S., and Van Halbeek, H. (1988) The asparagine-linked oligosaccharides on bovine fetuin. Structural analysis of N-glycanase-released oligosaccharides by 500-megahertz 1H NMR spectroscopy. *J. Biol. Chem.* **263**, 18253–18268
36. Uozumi, N., Yanagidani, S., Miyoshi, E., Ihara, Y., Sakuma, T., Gao, C. X., Teshima, T., Fujii, S., Shiba, T., and Taniguchi, N. (1996) Purification and cDNA cloning of porcine brain GDP-L-Fuc:N-acetyl-β-D- glucosaminide α1→6Fucosyltransferase. *J. Biol. Chem.* **271**, 27810–27817
37. Wang, X., Inoue, S., Gu, J., Miyoshi, E., Noda, K., Li, W., Mizuno-Horikawa, Y., Nakano, M., Asahi, M., Takahashi, M., Uozumi, N., Ihara, S., Lee, S. H., Ikeda, Y., Yamaguchi, Y., *et al.* (2005) Dysregulation of TGF-β1 receptor activation leads to abnormal lung development and emphysema-like phenotype in core fucose-deficient mice. *Proc. Natl. Acad. Sci. U. S. A.* **102**, 15791–15796
38. Yang, Q., Zhang, R., Cai, H., and Wang, L. X. (2017) Revisiting the substrate specificity of mammalian α1,6-fucosyltransferase reveals that it catalyzes core fucosylation of N-glycans lacking α1,3-arm GlcNAc. *J. Biol. Chem.* **292**, 14796–14803
39. Van Meel, E., Lee, W. S., Liu, L., Qian, Y., Doray, B., and Kornfeld, S. (2016) Multiple domains of GlcNAc-1-phosphotransferase mediate recognition of lysosomal enzymes. *J. Biol. Chem.* **291**, 8295–8307
40. Vaughn, D. E., Rodriguez, J., Lazebnik, Y., and Joshua-Tor, L. (1999) Crystal structure of Apaf-1 caspase recruitment domain: An α-helical Greek key fold for apoptotic signaling. *J. Mol. Biol.* **293**, 439–447
41. Van Dijk, W., Havenaar, E. C., and Brinkman-Van Der Linden, E. C. M. (1995) α1-Acid glycoprotein (orosomucoid): Pathophysiological changes in glycosylation in relation to its function. *Glycoconj. J.* **12**, 227–233
42. Coddeville, B., Carchon, H., Jaeken, J., Briand, G., and Spik, G. (1998) Determination of glycan structures and molecular masses of the

glycovariants of serum transferrin from a patient with carbohydrate deficient syndrome type II. *Glycoconj. J.* **15**, 265–273

43. Oury, T. D., Crapo, J. D., Valnickova, Z., and Enghild, J. J. (1996) Human extracellular superoxide dismutase is a tetramer composed of two disulphide-linked dimers: A simplified, high-yield purification of extracellular superoxide dismutase. *Biochem. J.* **317**, 51–57
44. Kuwabara, N., Manya, H., Yamada, T., Tateno, H., Kanagawa, M., Kobayashi, K., Akasaka-Manya, K., Hirose, Y., Mizuno, M., Ikeguchi, M., Toda, T., Hirabayashi, J., Senda, T., Endo, T., and Kato, R. (2016) Carbohydrate-binding domain of the POMGnT1 stem region modulates O-mannosylation sites of α-dystroglycan. *Proc. Natl. Acad. Sci. U. S. A.* **113**, 9280–9285
45. Xiong, H., Kobayashi, K., Tachikawa, M., Manya, H., Takeda, S., Chiyonobu, T., Fujikake, N., Wang, F., Nishimoto, A., Morris, G. E., Nagai, Y., Kanagawa, M., Endo, T., and Toda, T. (2006) Molecular interaction between fukutin and POMGnT1 in the glycosylation pathway of α-dystroglycan. *Biochem. Biophys. Res. Commun.* **350**, 935–941
46. Emsley, P., and Cowtan, K. (2004) Coot: Model-building tools for molecular graphics. *Acta Crystallogr. D Biol. Crystallogr.* **60**, 2126–2132
47. Kabsch, W. (1976) A solution for the best rotation to relate two sets of vectors. *Acta Cryst.* **A32**, 922–923
48. Okamoto, R., Mandal, K., Sawaya, M. R., Kajihara, Y., Yeates, T. O., and Kent, S. B. H. (2014) (Quasi-)racemic X-ray structures of glycosylated and non-glycosylated forms of the chemokine Ser-CCL1 prepared by total chemical synthesis. *Angew. Chem. Int. Ed. Engl.* **53**, 5194–5198
49. Nakano, M., Saldanha, R., Göbel, A., Kavallaris, M., and Packer, N. H. (2011) Identification of glycan structure alterations on cell membrane proteins in desoxyepothilone B resistant leukemia cells. *Mol. Cell. Proteomics* **10**. M111.009001